Original Article

MOLECULAR METABOLISM

Aberrant overexpression of *HOTAIR* inhibits abdominal adipogenesis through remodelling of genome-wide DNA methylation and transcription

Feng-Chih Kuo [1,*], Yu-Chun Huang [2,3,4], Ming-Ren Yen [2], Chien-Hsing Lee [1], Kuo-Feng Hsu [5], Hsiang-Yu Yang [6], Li-Wei Wu [7,8], Chieh-Hua Lu [1], Yu-Juei Hsu [9], Pao-Yang Chen [2,3,]**

ABSTRACT

Objective: Abdominal adiposity is strongly associated with diabetic and cardiovascular comorbidities. The long noncoding RNA *HOTAIR* (HOX Transcript Antisense Intergenic RNA) is an important epigenetic regulator with fat depot-specific expression. Its functional roles and epigenetic regulation in abdominal adipogenesis remain uncertain.

Methods: We collected different fat depots from healthy, severely obese, and uraemic subjects to measure fat-depot specific gene expression and quantify regional adiposity via dual-energy X-ray absorptiometry (DXA). *HOTAIR* was overexpressed to evaluate its functional roles. Reduced representation bisulfite sequencing (RRBS), RNA-sequencing, real-time qPCR and RNA/chromatin immunoprecipitation were performed to analyse *HOTAIR*-mediated epigenetic regulation.

Results: A negative correlation between adipose tissue *HOTAIR* expression (arm or abdominal subcutaneous fat depots) and regional adiposity under the status of severe obesity or uraemia was observed. *HOTAIR* overexpression using human immortalized abdominal preadipocytes further revealed its anti-adipogenic effects. Integrative analysis of genome-wide DNA methylation by reduced representation bisulfite sequencing (RRBS) and gene expression was performed. Overall, the differentially methylated genes were functionally enriched for nervous system development, suggesting that *HOTAIR* may be epigenetically associated with cell lineage commitment. We specifically found that *HOTAIR*-mediated genes showed strong changes in both DNA methylation and gene expression during abdominal adipogenesis. We observed that two *HOTAIR*-repressed genes, *SLITRK4* and *PITPNC1,* present an obesity-driven fat-depot specific expression pattern that is positively correlated with the central body fat distribution.

Conclusions: Our study indicated that *HOTAIR* is a key regulator of abdominal adipogenesis via intricate DNA methylation and is likely to be associated with the transcriptional regulation of genes involved in nervous system development and lipid metabolism, such as *SLITRK4* and *PITPNC1*.

Keywords lncRNA; *HOTAIR*; Subcutaneous adipose tissue; Visceral adipose tissue; Abdominal adipogenesis; Epigenetic regulation; Nervous system development; Human body fat distribution; DNA methylation

1. INTRODUCTION

Obesity significantly increases the risks for cardiometabolic disorders, such as myocardial infarction and type 2 diabetes [1,2]. In addition to general adiposity and regional body fat distribution, central fat accumulation is an even stronger risk factor than obesity *per se* for triggering cardiovascular diseases [3,4]. Studies have revealed that upper-body fat and lower-body fat have different biological functions [5,6]. Lower-body fat, such as gluteofemoral subcutaneous adipose tissue (SAT), functions as a stable metabolic reservoir, which could maintain long-term fatty acid storage and expand healthily via predominant adipocyte hyperplasia. Upper-body fat, including abdominal SAT and visceral adipose tissue (VAT), presents dynamically quick uptake and rapid release of free fatty acids and tends to expand its

[1]Division of Endocrinology and Metabolism, Department of Internal Medicine, Tri-Service General Hospital, National Defense Medical Center, Taipei, Taiwan [2]Institute of Plant and Microbial Biology, Academia Sinica, Taipei, Taiwan [3]Bioinformatics Program, Taiwan International Graduate Program, National Taiwan University, Taipei, Taiwan [4]Bioinformatics Program, Institute of Information Science, Taiwan International Graduate Program, Academia Sinica, Taipei, Taiwan [5]Division of General Surgery, Department of Surgery, Tri-Service General Hospital, National Defense Medical Center, Taipei, Taiwan [6]Division of Cardiovascular Surgery, Department of Surgery, Tri-Service General Hospital, National Defense Medical Center, Taipei, Taiwan [7]Division of Family Medicine, Department of Family and Community Medicine, Tri-Service General Hospital, National Defense Medical Center, Taipei, Taiwan [8]Health Management Center, Department of Family and Community Medicine, Tri-Service General Hospital, National Defense, Medical Center, Taipei, Taiwan [9]Division of Nephrology, Department of Internal Medicine, Tri-Service General Hospital, National Defense Medical Center, Taipei, Taiwan

*Corresponding author. E-mail: shoummie@hotmail.com (F.-C. Kuo).

**Corresponding author. Institute of Plant and Microbial Biology, Academia Sinica, Taipei, Taiwan. E-mail: paoyang@gate.sinica.edu.tw (P.-Y. Chen).

Received December 9, 2021 • Revision received February 21, 2022 • Accepted March 8, 2022 • Available online 12 March 2022

https://doi.org/10.1016/j.molmet.2022.101473

storage capacity via adipocyte hypertrophy [5]. Hypertrophic adipocytes frequently induce a hypoxic microenvironment, increase the recruitment of macrophages, and subsequently induce hepatic and systemic insulin resistance with frequent lipid overspill to initiate the harmful atherosclerotic cascade [7]. Therefore, investigating the determinants for the regulation of regional adipocyte biology, such as abdominal adipogenesis, will help to identify novel therapeutic targets for ameliorating obesity-associated cardiovascular risks.

Recent research has shown that the functional discrepancy between upper-body and lower-body fat might stem from their distinct developmental origins with differential expression on several homeobox (HOX) genes [6,8–10]. In particular, *HOTAIR* (HOX Transcript Antisense Intergenic RNA), as a long noncoding RNA, is one of the most differentially expressed genes between abdominal and gluteal fat depots, and its expression level is much higher in gluteal SAT than in abdominal SAT [6]. *HOTAIR* resides within the *HOXC* locus (chromosome 12) and is well known as an important epigenetic regulator that causes chromatin silencing *in trans* at the *HOXD* locus (chromosome 2) by interacting with polycomb repressive complex 2 (PRC2), which contains histone methyltransferase EZH2 (enhancer of zeste homologue 2) at the 5′ end and lysine-specific histone demethylase 1 (LSD1) at the 3' end to modulate H3K27 trimethylation and H3K4 demethylation, respectively [11]. *HOTAIR* may be involved in adipocyte differentiation through various mechanisms mediated by these key epigenetic regulators. For instance, previous research has shown that LSD1 and EZH2 of PRC2 could regulate adipogenesis by demethylating H3K4 and inducing H3K27me3, respectively, on the promoter regions of the Wnt signalling genes [12,13]. *HOTAIR* is also highly dysregulated among various cancers and could possibly epigenetically regulate hundreds of genes to promote carcinogenesis, cell proliferation, or tumour metastases [14,15]. Moreover, *HOTAIR* is sited near the *HOXC13* locus, which is one of the genome-wide association studies (GWAS) that identified loci for human fat distribution [16]. Taken together, *HOTAIR* is very likely a functional epigenetic regulator to maintain or regulate the transcriptome profile in regional adipose tissue and plays a critical role in adipocyte biology, such as abdominal adipogenesis.

Histone modifications might alter chromatin accessibility for transcription factors to influence genetic transcription [17]. Recent studies suggest that *HOTAIR* also modulates DNA methylation on the promoter regions of specific genes, such as *PTEN* and *PCDH10* [18,19]. In addition, *PTEN* and *PCDH10* could inhibit the PI3K/Akt signalling pathway, which is known to play important roles in adipogenesis [20,21]. Considering that *HOTAIR*-related epigenetic modifications might present cellular-specific properties, we aim to utilize human immortalized abdominal preadipocytes to decipher *HOTAIR*-regulated temporal genome-wide DNA methylation and transcriptional patterns during abdominal adipocyte differentiation.

Currently, only a few studies have investigated the expression of the *HOTAIR* gene in human adipose tissue, and they merely studied abdominal or gluteal SAT in healthy individuals [6,22]. We hypothesized that *HOTAIR* expression in adipose tissue might be dysregulated under metabolic or inflammatory conditions and might subsequently influence regional adiposity, such as in patients with severe obesity or end stage renal disease (ESRD). Therefore, we conducted the 1st Asian study comparing *HOTAIR* expression in different fat depots from healthy, severely obese, or uraemic patients; examined the correlation between expression levels and regional adiposity; induced *HOTAIR* overexpression in the human abdominal preadipocyte cellular model to assess its phenotypic effects and epigenetic regulation; and linked the *HOTAIR*-repressed genes to the obesity-driven human body fat distribution.

2. RESULTS

2.1. *HOTAIR* was differentially expressed among different fat depots and might be modulated under the status of severe obesity or uraemia to influence human body fat distribution

In line with previous reports [6,22], we observed that *HOTAIR* is also highly expressed in gluteal SAT among Asian subjects, whereas arm, abdominal and visceral SAT all showed low expression levels (Supplementary Figure 1), confirming that *HOTAIR* is critical in fat depot distribution. In particular, differential expression was observed in SAT between normal-weight individuals and severely obese or uraemic patients (Figure 1A). To be more specific, we found that abdominal SAT *HOTAIR* expression was suppressed in the status of severe obesity, whereas arm SAT *HOTAIR* expression could be aberrantly increased in the uraemic status (Figure 1A). Furthermore, SAT *HOTAIR* expression is negatively correlated with regional body fat percentage. The lower expression of abdominal SAT *HOTAIR* was correlated with increased abdominal adiposity in severely obese subjects, and a higher expression of arm SAT *HOTAIR* was found to be correlated with decreased arm adiposity in uraemic patients (Figure 1B). Using dual-energy X-ray absorptiometry (DXA) to precisely measure regional body fat composition, both severely obese and uraemic patients showed a higher android-to-gynoid fat ratio than normal-weighted individuals (Table 1). It is not surprising that central fat accumulation with metabolic disturbance (increase in systemic blood pressure, triglyceride, low-density lipoprotein, aspartate aminotransferase and uric acid and decrease in high-density lipoprotein) was observed in the obese patients, but it is worth noting that uraemic patients also present central obesity even under relatively low general adiposity (Table 1). These results suggest that *HOTAIR* levels might be dynamically changed under metabolic or inflammatory conditions with potential functional roles in regulating regional adiposity or human fat distribution.

2.2. *HOTAIR* overexpression remarkably inhibits *in vitro* abdominal adipogenesis

Since *HOTAIR* is located within the developmental HOXC gene cluster and functions as an epigenetic regulator [11,14], we hypothesized that its low expression in the abdominal/arm SAT might be an epigenetic memory mark for maintaining the biological function of regional adipose tissue. We conducted constitutive overexpression of *HOTAIR* using lentiviral transduction in immortalized human abdominal preadipocytes (Abd *HOTAIR-OE* cells), and an empty vector was used to generate Abd Control cells. The immortalized human abdominal preadipocyte cell line was derived from the abdominal SAT of a 50-year-old healthy male (BMI: 24.4 kg/m^2) and has been shown to be a useful cellular model to evaluate depot-of-origin adipocyte biological function [23]. First, we examined *HOTAIR* expression between Abd *HOTAIR-OE* cells and Abd Control cells during *in vitro* adipogenic differentiation and confirmed that Abd *HOTAIR-OE* cells presented persistently elevated levels of *HOTAIR* throughout the entire course of adipogenesis (Figure 1C). Time-course photograph and quantification of Oil red O staining showed that the Abd Control cells could differentiate well with abundant accumulation of lipid droplets, whereas adipogenic differentiation was significantly suppressed in the Abd *HOTAIR-OE* cells (Figure 1D). To determine whether *HOTAIR* influences the transcription of known adipogenic genes, we performed real-time qPCR on CCAAT enhancer binding protein alpha (*CEBP-α*) and peroxisome proliferator-activated receptor gamma (*PPAR-γ*), which are master regulator transcription factors for determining adipogenesis. The expression levels of these two genes in Abd *HOTAIR-OE* cells were also substantially inhibited during the entire course of adipogenic differentiation (Figure 1E), indicating that the

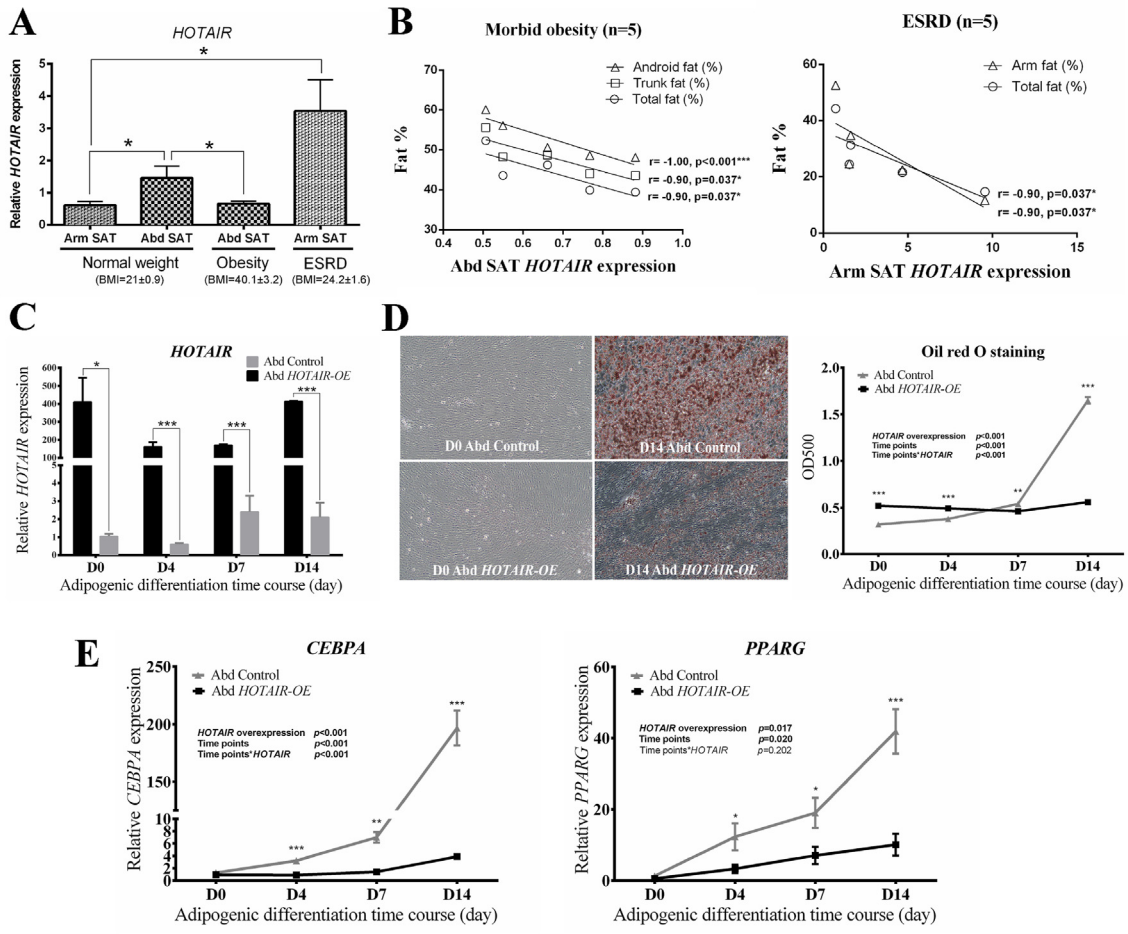

Figure 1: *HOTAIR* expression was dysregulated under the status of severe obesity or ESRD with anti-adipogenic effect during in vitro abdominal adipogenesis. (A) Paired arm subcutaneous adipose tissue (Arm SAT) and abdominal subcutaneous adipose tissue (Abd SAT) were collected from 6 healthy individuals. Abd SAT was collected from 5 severe obese individuals. Arm SAT was also collected from 5 patients with end stage renal disease (ESRD). *HOTAIR* expression in different fat depots was measured. **(B)** Body composition and regional adiposity were measured via Dual-energy X-ray Absorptiometry (DXA). **(C)** The immortalized human abdominal preadipocyte cell line derived from abdominal subcutaneous adipose tissue was used to assess human regional adipocyte biology. Constitutive *HOTAIR* overexpression (Abd *HOTAIR-OE* cell) was conducted via lentiviral transduction and empty vector was used to generate the Abd Control cell. *In vitro* adipogenesis of Abd *HOTAIR-OE* and Abd Control cells were performed and *HOTAIR* expression was measured during adipogenic differentiation (n = 3). **(D)** The status of lipid droplet formation was quantified with Oil red O staining during adipogenic differentiation (n = 3) and cells were photographed on D0 and D14 (x200 magnification). **(E)** The expression of two master regulator transcription factors (*CEBPA* and *PPARG*) for adipocyte differentiation was measured during adipogenic differentiation (n = 3). All data are presented as means ± SEM. Gene expression was measured via real-time qPCR. Statistical significance was assessed using independent Student T-test to compare different fat-depots or two cells at the same time point & two-way ANOVA to evaluate the effects of two factors (*HOTAIR* overexpression & time points). The correlation between regional adiposity and the *HOTAIR* expression in regional adipose tissue was assessed with Spearman's correlation test, $*p < 0.05$; $**p < 0.01$; $***p < 0.001$.

aberrant overexpression of *HOTAIR* largely impedes the normal process of *in vitro* abdominal adipogenesis.

2.3. *HOTAIR* overexpression during abdominal adipogenesis increases global CG methylation and maintains the methylation status of genes functionally enriched for neural development

The process of *HOTAIR*-mediated epigenetic regulation through chromatin modifications, such as modulating H3K27me3 and demethylating H3K4 by recruiting PRC2 and LSD1 to the target genes and repressing their expression, has been widely acknowledged [11,14,24,25]. However, *HOTAIR* is a fat-depot-specific long non-coding RNA, and it is still unknown whether *HOTAIR* can regulate DNA methylation, particularly in preadipocytes or differentiated adipocytes. To comprehensively understand *HOTAIR*-mediated epigenetic regulation via DNA methylation during adipose differentiation, we performed reduced representation bisulfite sequencing (RRBS) among Abd *HOTAIR-OE* and Abd Control cells to unbiasedly assess genome-wide DNA methylation on differentiation day 0 and day 14. The mapping statistics of RRBS data were analysed with a minimum 4x reading depth (Table 2). A heatmap of methylomes was plotted to visualise the methylation levels and the correlation among these methylomes. Clearly, the methylomes of Abd *HOTAIR-OE* and Control cells were separated into two groups (Supplementary Figure 2A), and the metagene plot of methylation levels shows that transcription start sites have a significant dip, potentially to allow the binding of transcription factors (Supplementary Figure 2B). Then, principal component analysis (PCA) and two-way ANOVA of global CG methylation obviously showed that *HOTAIR* overexpression was the predominant effect among these methylomes, and time (day 0 and day 14) had a secondary effect that mainly influenced the methylation levels of control cells (Figure 2A and

Table 1 — Anthropometric and biochemical characteristics of the study population.

	Normal weight (n = 6, F:M = 6:0)	Morbid Obesity (n = 5, F:M = 2:3)	Uremia (n = 5, F:M = 3:2)
Age (years)	36.8 [24.7; 38.5]	31.1 [26.0; 39.3]	**66.0 [52.0; 71.2]***†
BMI (kg/m^2)	20.8 [19.3; 23.4]	**38.9 [34.9; 45.9]***	**24.6 [21.3; 26.9]**†
Waist-to-hip ratio	0.796 [0.757; 0.849]	**0.954 [0.878; 1.102]***	0.897 [0.859; 0.936]
Systolic BP (mmHg)	113.5 [111.3; 125.8]	**153 [142; 165.5]***	**149 [125.5; 158]***
Diastolic BP (mmHg)	71.5 [63.8; 77.8]	100 [78.5; 115.5]	73 [59.5; 96]
Fasting glucose (mg/dL)	87 [82.5; 89]	101 [85; 105.5]	100 [84; 120]
HbA1c (%)	5.35 [5.1; 5.6]	5.7 [5.3; 6.35]	5.8 [5.35; 6.8]
Triglyceride (mg/dL)	64 [54.5; 104.25]	**169 [106.5; 289.5]***	102 [81.5; 114]
HDL cholesterol (mg/dL)	66 [60.75; 74.25]	**46 [35; 50.5]***	**38 [27; 58]***
Total cholesterol (mg/dL)	175.5 [159.5; 180.25]	206 [160.5; 234]	**146 [117.5; 157.5]**†
LDL cholesterol (mg/dL)	93 [83.75; 108]	**135 [113.5; 168]***	**87 [50; 108.5]**†
BUN (mg/dL)	8.5 [8; 11]	14 [11; 19]	**74 [52; 104.5]***
Cr (mg/dL)	0.65 [0.48; 0.7]	0.9 [0.6; 1.3]	**10 [5.6; 11]***†
AST (U/L)	14 [13.25; 15.75]	**26 [20.5; 46.5]***	23 [16; 41]
ALT (U/L)	12 [9.5; 15.5]	61 [22.5; 115]	9 [5; 50]
Uric acid (mg/dL)	4.1 [3.45; 4.9]	**6.5 [6.25; 8.95]***	5.1 [3.9; 6.8]
DXA parameters			
Total body fat (%)	38.3 [31.8; 41.43]	43.6 [39.65; 49.25]	**24.4 [18.1; 37.75]**†
Trunk fat (%)	39.5 [31.55; 42.93]	48.2 [43.8; 52.15]	**27.9 [19.7; 36.4]**†
Android fat (%)	44.35 [33; 49.65]	50.6 [48.35; 58.1]	**32.5 [22.1; 39.9]**†
Gynoid fat (%)	47.35 [44.98; 50.45]	45.6 [41.95; 53.25]	29.4 [21.05; 42.45]
Arm fat (%)	36.6 [30.98; 43.63]	34.9 [33.2; 47.8]	24.5 [17; 43.65]
Android fat mass (kg)	1.46 [1.08; 1.89]	**4.53 [3.60; 8.19]***	**1.35 [0.92; 2.02]**†
Gynoid fat mass (kg)	3.72 [3.35; 5.03]	7.69 [7.23; 12.12]	**1.90 [1.46; 3.44]**†
Android/gynoid fat ratio§	0.371 [0.309; 0.422]	**0.603 [0.495; 0.683]***	**0.664 [0.555; 0.693]***

Data were analyzed using the Kruskal-Wallis one-way ANOVA with pairwise comparisons and are presented as median values and [quartiles]. Abbreviations: F, female; M, male; BMI, body mass index; BP, blood pressure; HbA1c, glycated hemoglobin; HDL, high-density lipoprotein; LDL, low-density lipoprotein; BUN, blood urea nitrogen; Cr, creatinine; AST, aspartate aminotransferase; ALT, alanine aminotransferase; DXA, dual-energy X-ray absorptiometry.
§: android/gynoid fat ratio was calculated via dividing android fat mass by gynoid fat mass.
*$p < 0.05$ as compared with normal weight group.
†$p < 0.05$ as compared between the Obesity and Uremia groups.
The bold word refers to variables with $p < 0.05$ as compared with the indicated group.

Table 2 — Mapping statistics of the RRBS data.

Sample name	Number of raw reads	Uniquely mapped reads	Mappability (%)	Depth[a] (X)
Day 0-HOTAIR-OE-1	267,058,158	151,599,008	56.77	28.38
Day 0-HOTAIR-OE-2	162,770,712	93,859,258	57.66	20.62
Day 0-control-1	137,163,220	71,441,736	52.09	16.22
Day 0-control-2	129,165,794	85,135,156	65.91	18.39
Day 14-HOTAIR-OE-1	125,431,522	78,341,008	62.46	15.69
Day 14-HOTAIR-OE-2	147,841,920	74,430,124	50.34	15.57
Day 14-control-1	158,658,448	90,837,542	57.25	18.01
Day 14-control-2	145,033,610	81,799,402	56.40	16.40

[a] The depth is counted by coverage of the RRBS-covered sites.

Table 3). *HOTAIR* overexpression also led to the union state of the methylome, while the methylomes of D0 and D14 control cells were diverse (Figure 2A). Direct comparison of the methylation status between Abd *HOTAIR-OE* and Abd Control cells revealed that *HOTAIR* overexpression significantly increased global CG methylation levels, particularly at day 0 (Figure 2B). Notably, the process of adipogenesis increased global CG methylation in Abd Control cells but had no effect on Abd *HOTAIR-OE* cells (Figure 2B).

To explore the effect of *HOTAIR-OE*-mediated DNA methylation at the gene level, we defined the *HOTAIR*-differentially methylated regions (DMRs) as △ CG methylation levels greater than or equal to 25% and t-test *p values* less than 0.05 between Abd *HOTAIR-OE* and control cells. If the DMRs overlap with gene bodies or promoters, these genes are deemed *HOTAIR*-mediated differentially methylated genes (*HOTAIR*-DMGs). We found that there were more *HOTAIR* hyper-DMGs at day 0, but after adipogenic differentiation (day 14), more hypo-DMGs were observed (Figure 2C). This time effect-related anti-correlation on *HOTAIR-DMGs* was mainly caused by the increase in global methylation in the control cells at day 14, as shown in Figure 2B. Furthermore, we examined the status of *HOTAIR* overexpression-mediated DMGs between differentiation day 0 and day 14, and it is intriguing that the majority (more than 84%) of gene body and promoter DMGs (both hyper- and hypo-) could maintain their methylation status (Figure 2D,E), suggesting that the methylation of these genes is constant and continuously affected by *HOTAIR*.

To understand the signalling pathways and molecular mechanisms associated with *HOTAIR*-mediated methylation during abdominal adipogenesis, we performed functional analysis using Ingenuity Pathway Analysis (IPA) software (https://www.qiagenbioinformatics.com/products/ingenuity-pathway-analysis) [26] on 540 constantly hypermethylated

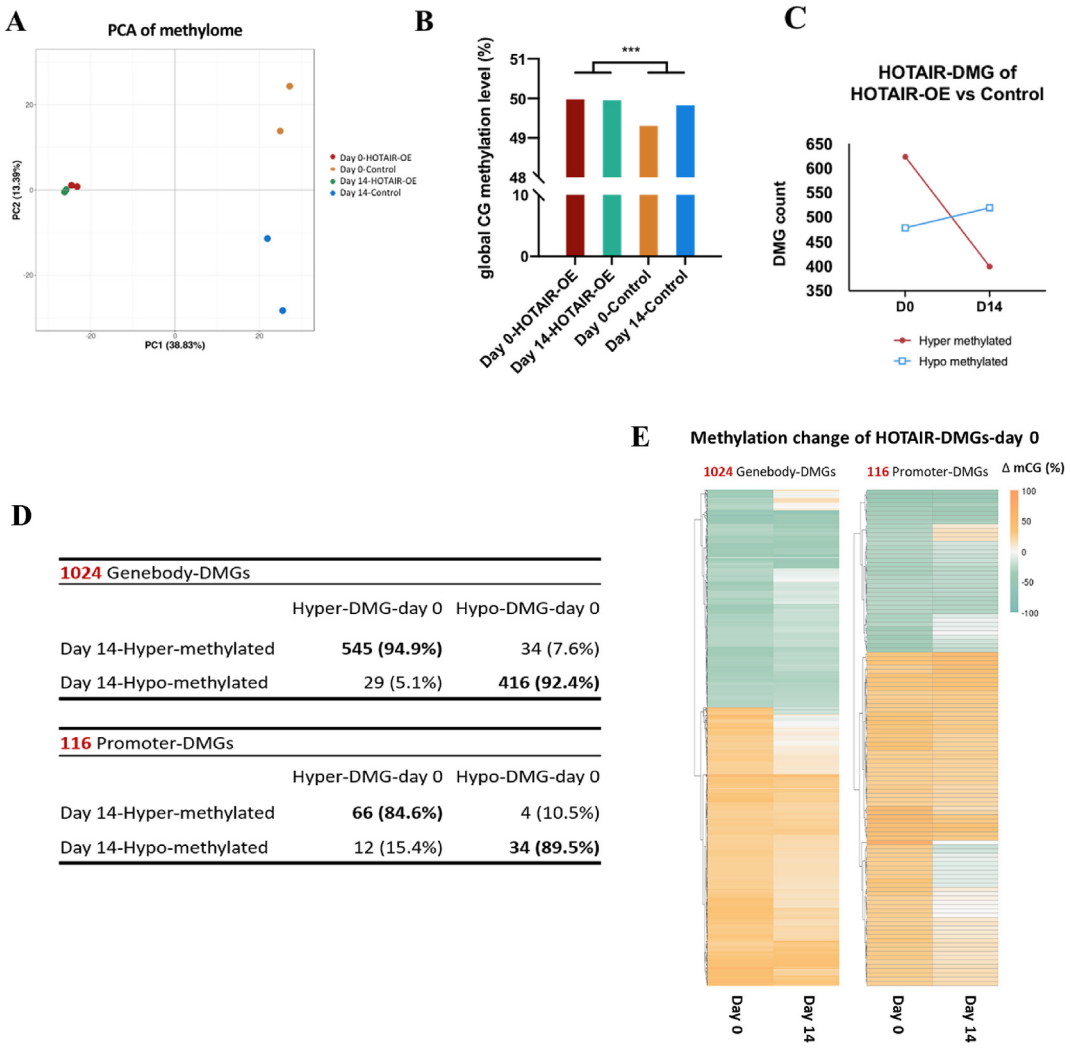

D

1024 Genebody-DMGs		
	Hyper-DMG-day 0	Hypo-DMG-day 0
Day 14-Hyper-methylated	**545 (94.9%)**	34 (7.6%)
Day 14-Hypo-methylated	29 (5.1%)	**416 (92.4%)**

116 Promoter-DMGs		
	Hyper-DMG-day 0	Hypo-DMG-day 0
Day 14-Hyper-methylated	**66 (84.6%)**	4 (10.5%)
Day 14-Hypo-methylated	12 (15.4%)	**34 (89.5%)**

Figure 2: Apply RRBS to analyze *HOTAIR* overexpression-mediated impact on genome-wide methylation during abdominal adipogenesis. (A) Principal component analysis (PCA) of methylome was performed among Abd *HOTAIR-OE* and Abd Control cells on adipogenic differentiation day 0 and day 14. **(B)** The global CG methylation levels of Abd *HOTAIR-OE* and Abd Control cells were compared. The global CG methylation between day 0-Control and day 14-Control also shows significant difference ($^{*}p < 0.05$; $^{**}p < 0.01$; $^{***}p < 0.001$). **(C)** The number counts of hyper- and hypo- differentially methylated gene (DMG) in *HOTAIR-OE* cell show significant difference on both day 0 and day 14 and present an anti-correlation with time effect. **(D, E)** The genebody- and promotor- DMGs in Abd *HOTAIR-OE* on day 0 and day 14 were compared, and the methylation status was plotted.

Table 3 — Numbers of CG methylated regions that were significantly affected by *HOTAIR* and developmental time using two-way ANOVA.

	HOTAIR	Developmental time	Interaction
CG regions[a]	5,289 (2,035)	—	—

The significant definition is $p < 0.05$ with Δ CG $\geq$ 20%.
[a] Parentheses indicate the affected genes.

DMGs and 400 constantly hypomethylated DMGs. The top 5 canonical pathways, molecular and cellular functions and physiological system development and function are shown in Supplementary Table 1A and 1B. Notably, both constantly hypermethylated and hypomethylated DMGs are functionally enriched for the same molecular and cellular functions, including "Cell-to-Cell Signalling and Interaction", "Cellular Assembly and Organization", "Cell Morphology", "Cellular Function and Maintenance" and "Cellular Development". Regarding physiological system development and function, both were mostly enriched for "Nervous System Development and Function". These results suggest that the biological function of Abd *HOTAIR-OE* preadipocytes was significantly altered and possibly deviated towards neural lineage cells. Moreover, the top canonical pathways are also associated with neuron or adipose tissue biology. The constantly hypermethylated DMGs were functionally enriched for "GABA Receptor Signalling", "Synaptogenesis Signalling Pathway" and "Endocannabinoid Neuronal Synapse Pathway". Then, the constantly hypomethylated DMGs were functionally enriched for "Netrin Signalling", "White Adipose Tissue Browning Pathway", "Axonal Guidance Signalling" and "CREB signalling in Neurons", indicating that the neurotransmitter signals within the Abd *HOTAIR-OE* preadipocytes were enhanced, which likely promoted adipose browning. Under the assumption that hypomethylated genes tend to be increased, we examined the predictive upstream and downstream signalling pathways regulated by the "White Adipose Tissue Browning Pathway"-associated constantly hypomethylated DMGs. Intriguingly, the functions of lipolysis and transdifferentiation

of white adipose tissue to beige adipose tissue were predicted to be activated accompanied by inhibition of white adipocyte differentiation (Supplementary Figure 3).

Taken together, our data suggest that genes involved in neural development and white adipose tissue browning are regulated by *HOTAIR* overexpression-mediated DNA methylation and that this alteration of neurometabolism during abdominal adipocyte differentiation may contribute to the anti-adipogenic effect of this gene.

2.4. *HOTAIR*-mediated differentially expressed genes are commonly maintained during abdominal adipogenesis with functions enriched in cellular movement and the cell cycle

To unbiasedly evaluate how *HOTAIR* overexpression influences the transcriptome, we performed RNA sequencing on both Abd *HOTAIR-OE* and Control cells at day 0, day 4, and day 14 of adipogenic differentiation. PCA disclosure time was the primary effect on the transcriptome, while within the same day, *HOTAIR* overexpression had a constant influence on the transcriptome to separate *HOTAIR-OE* and Control cells into two groups (Figure 3A). Since Abd *HOTAIR-OE* cells differentiated poorly as compared to Abd Control cells on differentiation day 14, it is not a surprise that these two cells have very different global transcription at this time point (Figure 3A). However, the PCA results of the methylome and transcriptome are very different, indicating that although *HOTAIR-OE* unifies the methylome, most of the gene expression is affected by the development time, not by their methylation status. Two-way ANOVA also showed that most of the gene expression was affected by the development time or the interaction effect of *HOTAIR* overexpression and development time, whereas 8,462 genes were directly associated with the *HOTAIR*-mediated methylation level (Supplementary Table 2). To examine whether the global transcription levels are influenced by the methylation status of the gene body or promoter, we further plotted the correlation between the methylation level and expression rank (Supplementary Figure 4A). Clearly, regardless of *HOTAIR* status or development time, gene methylation and expression show anti-correlations in promoters, whereas in the gene body, the anti-correlation is more obvious in highly expressed genes. These results support that the genes are globally repressed by high DNA methylation levels, and part of their expression is likely mediated by *HOTAIR* during adipogenesis.

Then, we defined the *HOTAIR*-mediated differentially expressed genes (*HOTAIR*-DEGs) as fold change less than −2 (downregulated) or more than 2 (upregulated) between Abd *HOTAIR-OE* and Control cells. Overall, there were slightly more downregulated DEGs than upregulated DEGs on day 0 (527 versus 514) but more upregulated DEGs than downregulated DEGs on day 4 (792 versus 637) and day 14 (2,382 versus 2,032) (Figure 3B). To specifically evaluate the transcriptome influenced by *HOTAIR* overexpression — not the developmental time — we particularly focused on the genes that were significantly dysregulated at day 0 of differentiation, as the dysregulation of genes could be more strongly associated with *HOTAIR*-mediated epigenetic regulation without interfering with the time effect of adipogenesis at later stages. Therefore, we further plotted the heatmap of expression fold change to visualize the dynamic change of day 0 *HOTAIR-DEGs* during adipogenesis day 4 and day 14 (Figure 3C). Intriguingly, among the 1,041 *HOTAIR*-DEGs at day 0, 27% (280 of 1,041) genes were constantly upregulated, and 19.9% (207 of 1,041) maintained downregulation. In total, almost half (46.8%) of day 0 *HOTAIR*-DEGs

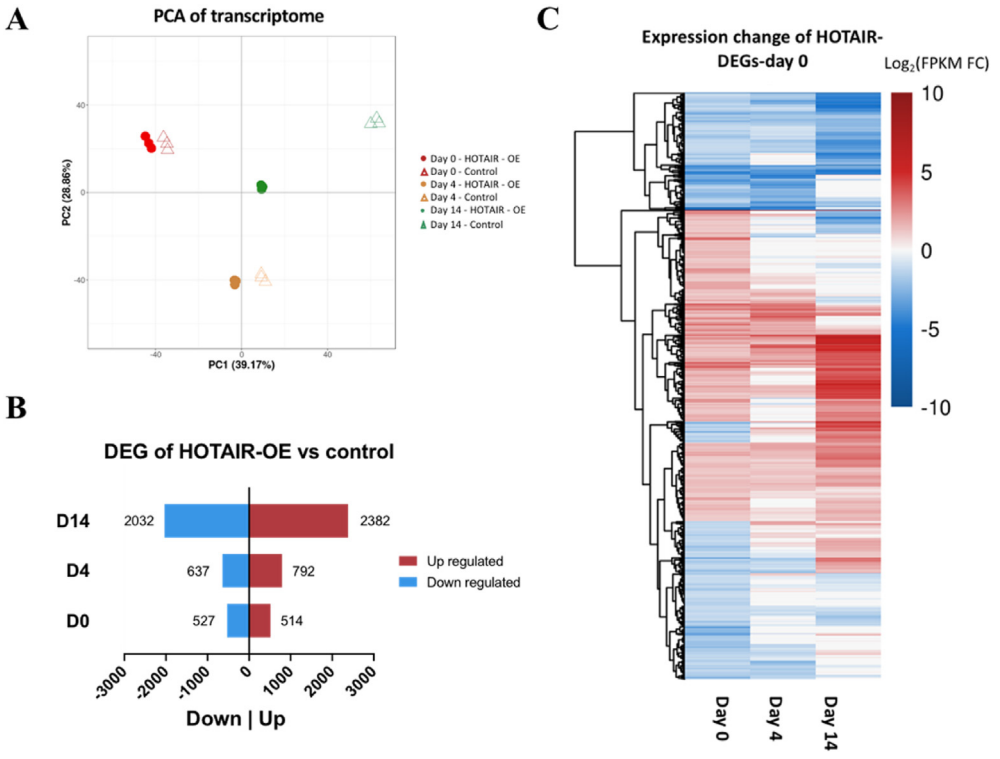

Figure 3: Apply RNA-sequencing to analyze *HOTAIR* overexpression-mediated impact on whole transcriptome during abdominal adipogenesis. (A) Principal component analysis (PCA) of transcriptome was performed among Abd *HOTAIR-OE* and Abd Control cells on adipogenic differentiation day 0 and day 14. **(B)** The numbers of up-/down-regulated differentially expressed genes (DEGs) in *HOTAIR-OE* cell on differentiation day 0, 4, and 14 were presented. **(C)** The transcriptional changes of DEGs-day 0 in *HOTAIR-OE* cell were shown from day 0 to day 4 and day 14.

maintained their regulated status on 4 and 14 (Supplementary Figure 4B), indicating that these genes are constantly regulated by *HOTAIR* throughout the entire course of adipogenesis.

We further performed IPA core analysis [26] on the 277 and 203 constantly upregulated and downregulated *HOTAIR*-DEGs to explore the signalling pathways and molecular mechanisms underpinning *HOTAIR*-mediated transcriptional regulation during abdominal adipogenesis. The top 5 canonical pathways, molecular and cellular functions and physiological system development and function are shown in Supplementary Table 3A and 3B. For the top canonical pathways in the constantly upregulated *HOTAIR*-DEGs, "Signalling by Rho Family GTPase" and "Regulation of Actin-based Motility by Rho" were predicted to be activated (positive Z-score), and "Rho GDI Signalling" as a downregulator of Rho family GTPase was shown to be inhibited (negative Z-score), indicating that the Rho proteins involved in intracellular actin dynamics were significantly activated. Additionally, "Cellular Movement" was listed as the top molecular and cellular function in the constantly upregulated DEGs (Supplementary Table 3A). Regarding the constantly downregulated *HOTAIR*-DEGs, "Cell Cycle" is listed at the top molecular and cellular functions. Additionally, analysis of the canonical pathways indicated that the "Kinetochore Metaphase Signalling Pathway" was inhibited (negative Z-score) and that "Cell Cycle: G2/M DNA Damage Checkpoint Regulation" was activated (positive Z-score), showing that mitosis of the cell cycle was suppressed (Supplementary Table 3B).

Overall, these data indicate that *HOTAIR* overexpression constantly regulates the transcriptome to enhance Rho protein-associated cytoskeletal dynamics and inhibit the mitotic progression of the cell cycle, which likely leads to *HOTAIR*-associated antiadipogenic effects during abdominal adipogenic differentiation.

2.5. Integrative analysis of *HOTAIR*-DEGs and *HOTAIR*-DMGs to identify downstream functional pathways and putative *HOTAIR*-regulated genes during abdominal adipogenesis

To examine whether the DEGs regulated by *HOTAIR-OE* are associated with DNA methylation, we analysed the corresponding promoter △ methylation levels of constantly up- and downregulated DEGs in *HOTAIR-OE* cells at day 0 and day 14 of adipogenesis (Figure 4A). Significantly, the methylation level of promoters of constantly downregulated DEGs increased, followed by their gene expression decreasing when *HOTAIR* was overexpressed. In contrast, the methylation level of promoters of constantly upregulated DEGs decreased, and their gene expression increased when *HOTAIR* was overexpressed. The constantly downregulated *HOTAIR*-DEGs had higher promoter CG methylation level changes than the constantly upregulated *HOTAIR*-DEGs, indicating that these *HOTAIR*-DEGs were

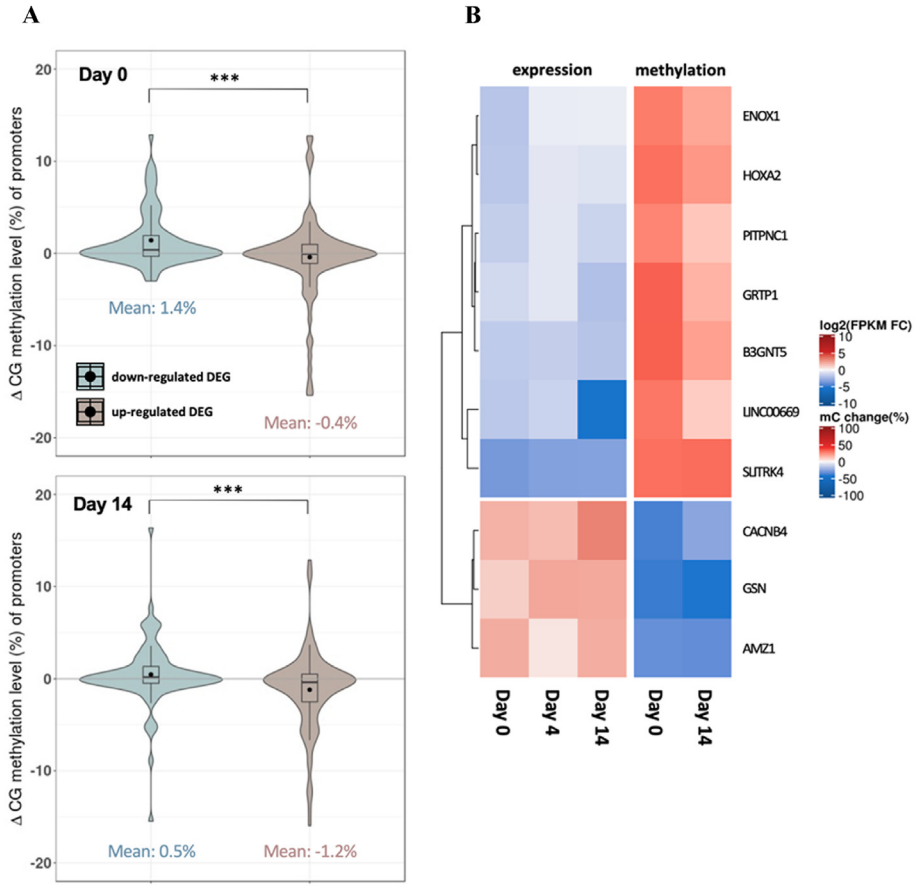

Figure 4: Combine RNA-sequencing and RRBS to identify putative functional genes or pathways regulated by *HOTAIR* during abdominal adipogenesis. (A) The corresponding promoter △ methylation levels of constantly up- and down-regulated DEGs in *HOTAIR-OE* cell were plotted at day 0 and day 14. The statistical significance was assessed using Student's t-test. $***p < 0.001$ **(B)** Within the day 0 DMG and DEG matched genes, there are 10 genes continuously maintain their methylation and corresponding expression status (7 for hyper-methylated and down-regulated, 3 for hypo-methylated and up-regulated) and were considered as the putative *HOTAIR*-regulated genes.

epigenetically regulated by DNA methylation at both day 0 and day 14 and that these genes were repressed by their promoter CG methylation level. Together, these findings emphasize that CG methylation mediated by *HOTAIR* reversely regulates gene expression.

Then, we performed IPA core analysis [26] on the 87 and 205 genes concurrently recognized as *HOTAIR-DEGs* and *HOTAIR-DMGs* at day 0 or day 14 to investigate the functional pathways and molecular mechanisms influenced by *HOTAIR*-associated epigenetic and transcriptional regulation during abdominal adipogenesis (Supplementary Table 4A and 4B). Notably, at day 0 and day 14, these genes were both functionally enriched for similar molecular and cellular functions, including "Cellular Assembly and Organization" and "Cellular Function and Maintenance". In terms of physiological system development and function, both of them were mostly enriched for "Nervous system Development and Function", which was the same as the enriched functions in *HOTAIR*-DMGs (Supplementary Table 1A and 1B). Additionally, some nervous system-associated signalling pathways are listed in the top canonical pathways, including "GABA Receptor Signalling" at day 0 and "Semaphorin Neuronal Repulsive Signalling Pathway" and "Synaptogenesis Signalling Pathway" at day 14 (Supplementary Table 4A and 4B). Again, this integrative analysis suggests that *HOTAIR* overexpression could modulate the cellular function of abdominal preadipocytes and likely increase their ability for adipose-neuron crosstalk or transdifferentiation.

To identify the genes most likely regulated by *HOTAIR*-mediated DNA methylation, we selected the day 0 *HOTAIR*-DMGs that were concurrently recognized as *HOTAIR*-DEGs with the correct corresponding direction, i.e., genes that were hypermethylated matched with downregulated genes and genes that were hypomethylated matched with upregulated genes. Then, we further pinpointed a total of 10 genes that continuously maintained their methylation and corresponding expression status at day 4 and day 14, as shown in Figure 4B. There were 7 hypermethylated and downregulated genes (*B3GNT5*, *ENOX1*, *GRTP1*, *LINC00669*, *PITPNC1*, *SLITRK4*, *HOXA2*) and 3 hypomethylated and upregulated genes (*AMZ1*, *CACNB4*, *GSN*). These putative *HOTAIR* epigenetically regulated genes may directly or indirectly influence abdominal adipogenesis.

Collectively, these results provide supportive evidence that *HOTAIR* overexpression during abdominal adipogenesis is associated with the anti-correlation between promoter CG methylation and gene expression and causes epigenetic and transcriptional alterations in the genes functionally enriched for cellular assembly and organization and nervous system development. Furthermore, 10 genes are epigenetically regulated by *HOTAIR* through DNA methylation during abdominal adipocyte differentiation. To prove their direct interactions with *HOTAIR* and potential functional roles in abdominal adipogenesis, we performed more experiments using abdominal preadipocytes for validation.

2.6. Validation of putative genes epigenetically suppressed by *HOTAIR* during abdominal adipogenesis

Among these 10 genes, 5 genes were selected for evaluation because their functions are associated with adipocyte differentiation, neuronal development or cellular assembly: *PITPNC1* is involved in lipid metabolism [27]; *SLITRK4* modulates synapse differentiation [28]; *ENOX1* regulates plasma membrane electron transport pathways [29]; *GRTP1* encodes a GTPase activator protein [30]; and gelsolin (*GSN*) is a key regulator of actin filament assembly [31]. We first measured their expression (*PITPNC1, SLITRK4, ENOX1, GRTP1 and GSN*) using real-time qPCR in Abd *HOTAIR-OE* and Control cells on day 0, 4, 7 and 14 of adipogenesis. Two genes (*SLITRK4 and PITPNC1*) were shown to be significantly suppressed throughout the whole course of adipogenesis in Abd *HOTAIR-OE* cells (Figure 5A). The other three genes (*ENOX1, GRTP1 and GSN*) presented compatible regulated transcriptional direction as the RNA-sequencing data but did not reach a significant difference in the whole course of differentiation (Supplementary Figure 5A). Therefore, we mainly focused on *SLITRK4* and *PITPNC1* to further explore *HOTAIR*-mediated chromatin modifications.

HOTAIR, as a long noncoding RNA with a secondary structure [32], has been shown to suppress its target genes by interacting with PRC2 at the 5′ end and LSD1 at the 3' end to modulate H3K27 trimethylation (from H3K27me2 to H3K27me3) and H3K4 demethylation (from H3K4me2 to H3K4me), respectively [11]. To examine whether *HOTAIR* could physically interact with PRC2 in the immortalized preadipocyte cell line, we performed RNA immunoprecipitation of EZH2, which is the functional enzymatic component of PRC2 as a methyltransferase [33]. Notably, after *HOTAIR* overexpression, the interaction between *HOTAIR* and EZH2 protein was significantly enhanced (Figure 5B), indicating that lncRNA-*HOTAIR* indeed interacts with PRC2 in abdominal preadipocytes. Subsequently, we performed chromatin immunoprecipitation using H3K27me3 antibody and ran real-time qPCR using the designed primers binding to the promoter region of the gene of interest. In Abd *HOTAIR-OE* cells, the occupancy of H3K27me3 was significantly enriched in the promoter region of *SLITRK4*, and there was a marginally significant increase ($p = 0.061$) in the promoter region of *PITPNC1* (Figure 5C), suggesting that *HOTAIR*-associated histone modifications work together with DNA hypermethylation to constantly suppress the transcription of *SLITRK4* and *PITPNC1*.

Since the *PPARG* expression of Abd *HOTAIR-OE* cells was also significantly and constantly inhibited throughout the course of adipogenesis (Figure 1E), we further performed H3K27me3 chromatin immunoprecipitation by running real-time qPCR targeting the *PPARG* promoter. Interestingly, we also observed that the occupancy of H3K27me3 on the promoter region of *PPARG* was significantly enhanced after *HOTAIR* overexpression (Figure 5C). This result indicates that some constantly downregulated *HOTAIR*-DEGs (such as *PPARG*) might be predominantly controlled by histone modifications without having significantly differential methylation status. Moreover, IPA upstream analysis of the constantly downregulated *HOTAIR*-DEGs showed that PPARG was a predicted upstream inhibitor (Z-score −1.79), leading to inhibition of molecules involved in the cell cycle (*CDKN2C*), lipid droplet formation (*PLIN4*) and fatty acid metabolism (*CD36 and LIPE*) (Figure 5D). These PPARG-associated networks provide a schematic view to explain how *HOTAIR* overexpression could possibly inhibit abdominal adipogenesis and will be warranted for further investigation.

2.7. Increased expression of Abd SAT *SLITRK4* and VAT *PITPNC1* is driven by obesity and positively correlated with central body fat distribution

After identifying *SLITRK4* and *PITPNC1* as *HOTAIR* epigenetically suppressed genes, we evaluated their potential functional roles in regional adipose tissue, particularly in abdominal or visceral fat depots. Therefore, we measured the transcriptional expression of these two genes at various fat depots among normal-weight individuals, subjects with severe obesity and uraemic patients. The results revealed that *SLITRK4* is specifically highly expressed in the abdominal SAT of patients with severe obesity. Additionally, VAT from severely obese patients presented significantly increased expression of *PITPNC1* (Figure 6A). In particular, the abdominal SAT *SLITRK4* and VAT *PITPNC1* levels were both positively correlated with the obesity-driven

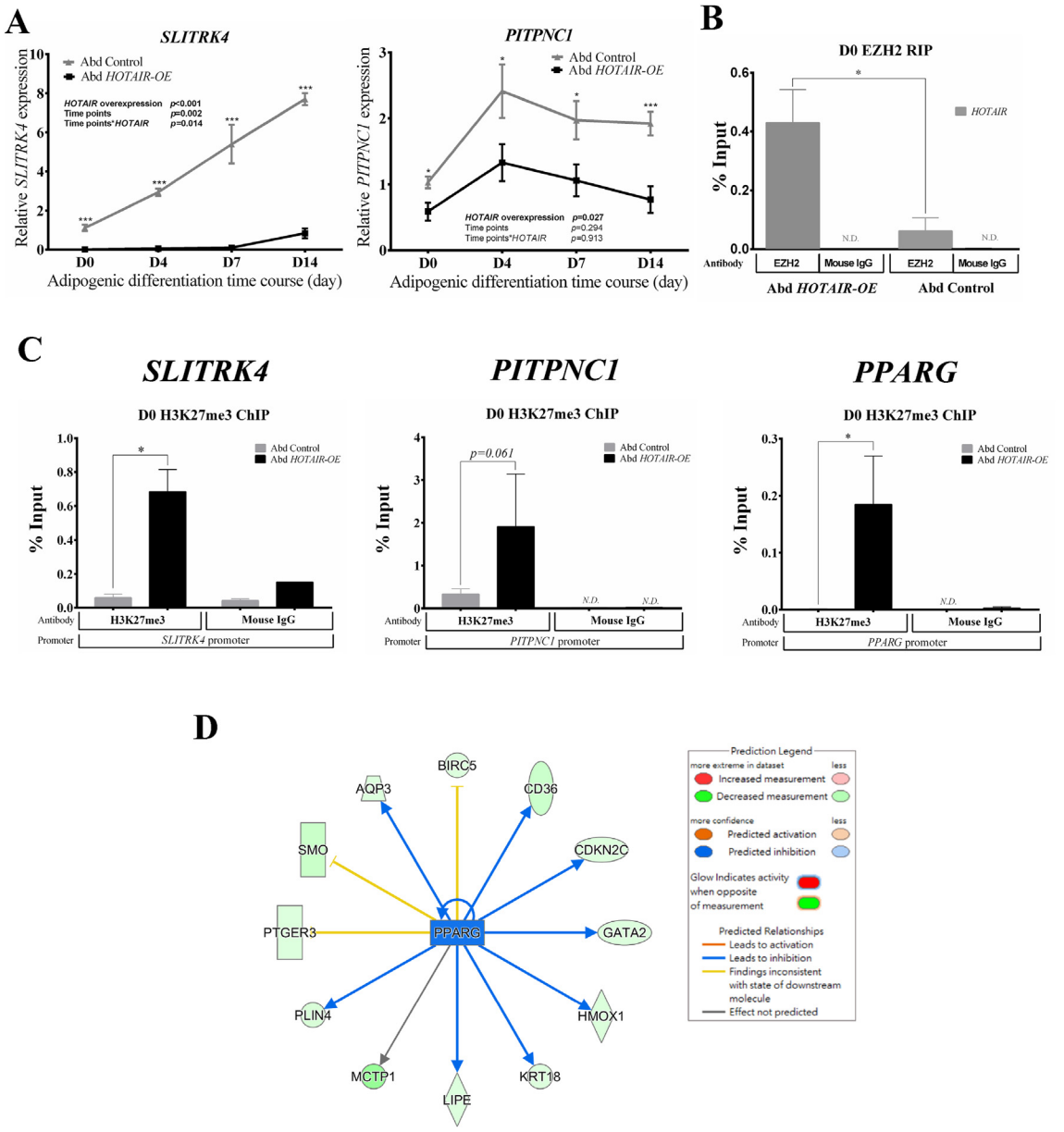

Figure 5: Validate the putative functional genes suppressed by *HOTAIR* using real-time qPCR, RNA immunoprecipitation (RIP) and chromatin immunoprecipitation (ChIP). (A) The expression of *SLITRK4* and *PITPNC1* on Abd *HOTAIR-OE* and Control cells during adipogenesis D0, D4, D7 and D14 was measured with real-time qPCR (n = 3). **(B)** RNA immunoprecipitation was performed via using EZH2 antibody in the D0 Abd *HOTAIR-OE* and Abd Control cells to evaluate the differential EZH2 interaction with *HOTAIR* between two cells (n = 5–6). **(C)** H3K27me3 chromatin immunoprecipitations were performed in the D0 Abd *HOTAIR-OE* and Abd Control cells to assess the differential chromatin occupancy on *SLITRK4*, *PITPNC1* and *PPARG* promoter regions between two cells (n = 3). Mouse IgG was used as the negative control. **(D)** IPA was performed on the constantly down-regulated DEGs in *HOTAIR-OE* cell and *PPARG* was listed as a predicted upstream inhibitor (Z-score −1.79), which leads to inhibition of several genes. All data are presented as means ± SEM. Statistical significance was assessed using independent Student's t-test to compare two cells at the same time point; two-way ANOVA to evaluate the effects of two factors (*HOTAIR* overexpression & time points) & Mann-Whitney U test to examine the differential %Input between two cells, $*p < 0.05$; $**p < 0.01$; $***p < 0.001$.

waist-to-hip ratio or DXA-quantified android-to-gynoid fat mass ratio (Figure 6B). This observational correlation suggests that these two genes/molecules might be functionally important for central fat accumulation and deserves future exploration.

3. DISCUSSION

Our results revealed that the long noncoding RNA *HOTAIR*, flanking by *HOXC11* and *HOXC12*, is differentially expressed in various adipose tissues and is highly expressed in gluteofemoral fat depot but maintains low levels in the arm and abdominal and visceral fat depots. This body position-specific *HOTAIR* expression follows similar rules as the HOX clusters. HOX genes are numbered 1 to 13 from the 3′ end to the 5' end of the gene sequence in the chromosome [34] and present collinearity with the same order of their expression along the anterior-posterior body axis [35,36]. HOX genes are known to be functionally important to ensure the development of correct structures in the correct places of the body during embryogenesis. Therefore, we

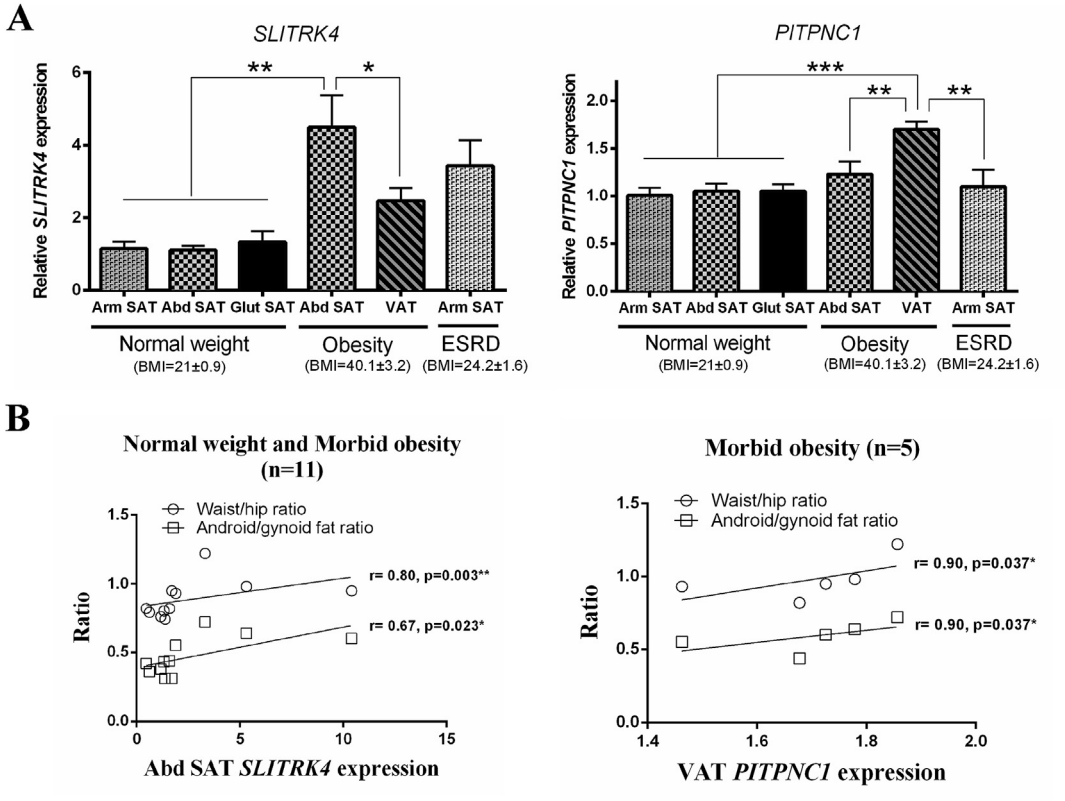

Figure 6: *SLITRK4* and *PITPNC1* as *HOTIAR* suppressed genes were, respectively, differentially expressed in abdominal SAT and VAT in the status of obesity and positively correlated with central body fat distribution. (A) Paired arm subcutaneous adipose tissue (Arm SAT), abdominal subcutaneous adipose tissue (Abd SAT) and gluteal subcutaneous adipose tissue (Glut SAT) were collected from 6 healthy individuals during cosmetic surgery. Paired Abd SAT and visceral adipose tissue (VAT) were collected from 5 morbidly obese individuals during bariatric surgery. Arm SAT was also collected from 5 patients with end stage renal disease (ESRD) as preparing the arteriovenous shunt. *SLITRK4* and *PITPNC1* expression in different fat depots was measured with real-time qPCR. Data presented as means ± SEM. Statistical significance was assessed using independent Student's t-test, $*p < 0.05$; $**p < 0.01$; $***p < 0.001$. **(B)** Body composition and regional adiposity were measured via Dual-energy X-ray Absorptiometry (DXA). Waist circumference and hip circumference were measured to the nearest 0.1 cm. Waist-to-hip ratio & android fat-to-gynoid fat ratio were used as two major surrogates to present the central body fat distribution. The correlation between central body fat distribution and Abd SAT *SLITRK4* and VAT *PITPNC1* expression was assessed with Spearman's correlation test, $*p < 0.05$; $**p < 0.01$; $***p < 0.001$.

hypothesize that *HOTAIR* is an important epigenetic regulator for controlling or maintaining the biological function of regional adipose tissue and might be altered under metabolic or inflammatory conditions. Indeed, we observed that abdominal SAT *HOTAIR* expression was further inhibited under severe obesity and that arm SAT *HOTAIR* levels were significantly enhanced in uraemic patients. Using human immortalized abdominal preadipocytes, we revealed that *HOTAIR* overexpression significantly inhibited *in vitro* abdominal adipogenesis, consistent with our observation that *HOTAIR* levels were negatively correlated with abdominal adiposity. However, this is contrary to another report that ectopic *HOTAIR* overexpression was shown to enhance abdominal adipogenesis using primary abdominal preadipocytes [22]. The incompatible results might be due to different tissue contexts or experimental protocols. Nevertheless, considering that intrinsic *HOTAIR* expression in abdominal subcutaneous adipose tissue is low, particularly in severe obesity, our finding that aberrant *HOTAIR* overexpression remarkably suppresses abdominal adipogenesis appears more reasonable.

In our experiments, we conducted aberrant overexpression (around 200 to 400-fold) of *HOTAIR* in the immortalised abdominal preadipocyte and observed a strong anti-adipogenic effect during abdominal adipogenesis. However, there may be a concern whether the very high *HOTAIR* levels could interfere the normal process of adipogenesis. To examine this possibility, we also generated Glut Control and Glut *HOTAIR-OE* cells using the paired immortalised gluteal preadipocytes [23]. Notably, on adipogenesis day 14, the *HOTAIR* expression in Glut *HOTAIR-OE* cells also reached around 200-fold increase, but the Glut *HOTAIR-OE* cells could still differentiate adequately with similar *PPARG* expression comparing to that in Glut Control cells (Supplementary Figure 6). These data indicated that *HOTAIR* overexpression presents abdominal fat depot-specific anti-adipogenesis and strengthen the interests to explore the underpinned mechanisms in this study.

HOTAIR-mediated histone modifications have been widely approved, but they have mainly been studied in the field of cancers. Our results further demonstrate that *HOTAIR*-mediated epigenetic regulation is also present in adipose tissue. However, *HOTAIR*-mediated epigenetic regulation is not limited to histone modifications. Studies have shown that it can sponge many microRNAs to modulate multiple biological or pathological functions during embryonic development, cancer and human diseases [37]. It was also found to induce promoter hypermethylation with transcriptional silencing of tumour suppressing genes, such as *PTEN* [19]. *HOTAIR* is also involved in posttranslational modifications, such as protein degradation (ubiquitination) [38], NF-κB inflammatory pathways [39], and the process of DNA repair or the cell cycle [40]. In this study, we mainly focused on exploring *HOTAIR*-

mediated global methylation and its links with the regulation of the whole transcriptome by conducting integrative analysis of RRBS and RNA sequencing. We found that *HOTAIR* overexpression has a major impact on the adipocyte CG methylome; yet, the development time has more effects on gene expression. Additionally, *HOTAIR* overexpression constantly and concurrently influenced the methylation and transcriptional status of genes functionally enriched for "Nervous System Development and Function" during abdominal adipogenesis (Supplementary Table 1A, 1B, 3B, 4A, 4B). More intriguingly, the constantly hypomethylated DMGs were further enriched for the "White Adipose Tissue Browning Pathway" (Supplementary Table 1B and Supplementary Figure 3). It seems that these genes associated with nervous system development might play crucial roles in regulating the adipocyte biology of abdominal fat depots and could be largely controlled by *HOTAIR*-mediated CG methylation changes. Recent studies have revealed that human adipose tissue-derived stem cells can be transdifferentiated into neuron-like cells *in vitro* [41]. Additionally, adipose tissue can release signalling factors to local sensory fibres that convey to the central nervous system to regulate systemic metabolism, and adipose tissue is innervated by sympathetic nerves that regulate lipolysis and thermogenesis [42,43]. Therefore, it will be worth examining in the future whether *HOTAIR* overexpression could prompt abdominal adipose tissue towards beiging or browning, especially under stimulation with β3-adrenergic receptor agonists or cold exposure.

Regarding the *HOTAIR*-DEGs, we found that 46.8% of D0 DEGs in Abd *HOTAIR-OE* cells could be maintained as constantly upregulated or downregulated throughout the course of abdominal adipogenesis. Additionally, the promoter △ methylation levels of constantly downregulated *HOTAIR*-DEGs were significantly higher than those in the constantly upregulated *HOTAIR*-DEGs at day 0 and day 14, indicating that the DEGs in Abd *HOTAIR-OE* cells were constantly regulated by the differential methylation levels even though the absolute levels of difference were less than 2% (Figure 4A). These *HOTAIR-DEGs* not only have an anti-correlation with CG methylation but also may be regulated by other *HOTAIR*-mediated epigenetic mechanisms, such as changes in nuclear architecture or 3D chromatin structure/chromosome positions [44], histone modifications [11] or microRNA sponging [37], and have not been globally examined in our cells. However, we analysed the overall impacts of *HOTAIR* overexpression on the transcriptome of abdominal preadipocytes and highlighted that the molecular and cellular functions of "Cellular Movement" and "Cell Cycle" were most enriched for the constantly upregulated *HOTAIR*-DEGs and downregulated *HOTAIR*-DEGs, respectively. Our findings are in line with previous reports that the actin cytoskeleton and Rho pathway have been shown to be key regulators of adipogenic differentiation [45], and cellular proliferation during initial adipogenic differentiation is important for increasing the number of cells committed to adipocytes [46]. By combining RRBS analysis and RNA sequencing, we identified 10 genes heavily controlled by DNA methylation-mediated transcriptional regulation that maintained the same direction of change throughout the whole course of adipogenesis. Among them, we further identified two genes (*SLITRK4* and *PITPNC1*) that are regulated not only by *HOTAIR*-mediated changes in DNA methylation but also by histone modifications to maintain their constantly repressed expression during *in vitro* abdominal adipogenesis in Abd *HOTAIR-OE* cells. In addition to *HOTAIR*-mediated modifications of H3K27me3, we also examined its regulation of H3K4me2 by performing chromatin immunoprecipitation (Supplementary Figure 5B). Our results showed that the occupancies of H3K4me2 on the *SLITRK4*, *PITPNC1* and *PPARG* promoter regions were significantly increased in Abd *HOTAIR-OE* cells, which is opposite to our prediction since the *HOTAIR*-LSD1 complex was supposed to specifically demethylate mono- and dimethylation of H3K4 [11]. One possible explanation is that another histone demethylase rather than LSD1 might interact with *HOTAIR* to induce demethylation of H3K4me3 in abdominal preadipocytes.

To extend our *in vitro* findings of *HOTAIR*-mediated epigenetic modification to the *in vivo* situation of adipose tissue, we further measured *SLITRK4* and *PITPNC1* levels among various fat depots. When we compared their expression with *HOTAIR*, only *SLITRK4* showed a clear negative correlation among abdominal SATs between normal-weighted and obese subjects (Figure 1A and Figure 6A). Due to the incompletely matched results, we further examined two other genes *PPARG* and *PCDH10* that had been shown to be suppressed by *HOTAIR* in our *in vitro* cellular model and the previous report [18], respectively. As a result, *PCDH10* transcription was significantly enhanced in the obese abdominal SAT, whereas *PPARG* expression was significantly suppressed (Supplementary Figure 7A). The increased *PCDH10* expression in the low *HOTAIR*-expressed obese abdominal SAT supports that *HOTAIR* mediated epigenetic regulation also exhibits *in vivo*. Regarding to the *PPARG* gene, *PPARG* expression has been shown to be inhibited in the obese abdominal SAT [47], that our findings are in line with this observation. Moreover, recent studies revealed that *PPARG* levels were remarkably suppressed under the status of insulin resistance [48] and that the cytokines released by pro-inflammatory macrophages can inhibit the transcription of *PPARG* [49]. Hence, it is likely that, in the obese abdominal SAT, *HOTAIR* is not the sole factor to regulate the gene expression. The other factors may include the inflammatory microenvironment, insulin resistance and interactions between the diverse cell types within adipose tissue (adipocytes, preadipocytes, macrophages, neutrophils, lymphocytes, and endothelial cells) could all influence the gene transcription, particular the adipogenesis or lipid metabolism associated genes, such as *PPARG* and *PITPNC1*. Even though, the potential functional roles of *SLITRK4* and *PITPNC1* in abdominal adipocyte biology were still supported by their dynamically increased expression during adipogenesis, as observed in the well-differentiated Abd Control cells (Figure 5A). Moreover, their levels in the abdominal or visceral fat depots were shown to be positively correlated with obesity-driven apple-shaped body figures. Therefore, *SLITRK4* and *PITPNC1* are proposed to play important roles in inducing obesity-associated central fat accumulation. To date, few studies have focused on these two genes, and their functional characteristics in central obesity or regional adipose biology have yet to be fully elucidated.

The *SLITRK4* (SLIT and NTRK-like family, member 4) gene, located on chromosome X, encodes a transmembrane protein belonging to the Slitrk family. These family members contain two N-terminal leucine-rich repeat extracellular domains resembling those found in the axonal growth-controlling protein Slit, as well as a conserved intracellular C-terminal region similar to the neurotrophin receptor tropomyosin-related kinase (Trk). These proteins were named Slitrks due to their similarity with Slits and Trks [28]. *SLITRK4* is highly expressed in the adrenal gland and cerebellum, whereas adipose tissue is also listed as the 3rd rank of tissue with high *SLITRK4* expression based on Human Protein Atlas GTEx (Genotype-Tissue Expression) data (RNA-seq data on RSEMv1.2.22 (v7)). Genetic mutations in Slitrks have been associated with several neuropsychiatric disorders, such as obsessive-compulsive disorder [28], schizophrenia or Tourette syndrome [50], suggesting that Slitrks play prominent roles in normal nervous system development. Regarding *SLITRK* expression in regional adipose tissue, only one study found that *SLITRK* expression is higher in normal breast tissue than in breast carcinoma and is

associated with high serum oestradiol levels in an age-, menopausal-, or hormone therapy-dependent manner [51]. Our study is the first to report that *SLITRK4* was highly expressed in abdominal subcutaneous adipose tissue, positively correlated with central obesity, and epigenetically suppressed by *HOTAIR* during *in vitro* abdominal adipogenesis. These findings suggest that low levels of *HOTAIR* in abdominal subcutaneous adipose tissue are required for the increase in *SLITRK4*, which promotes the development of central fat accumulation. However, the detailed cellular and molecular mechanisms mediated by *SLITRK4* in abdominal fat depot are still largely unknown. The phosphatidylinositol transfer protein, cytoplasmic 1 (PITPNC1) gene, located on chromosome 17, encodes the PITPNC1 protein belonging to the phosphatidylinositol transfer protein (PITP) family. PITPs can mobilize phosphatidylinositol (PI) from the endoplasmic reticulum to the resident kinase for phosphorylation and are involved in multiple cellular processes, including cell signalling, membrane trafficking, cytoskeletal remodelling, and lipid metabolism [27]. *PITPNC1* was ubiquitously expressed in multiple tissues, with adipose tissue ranked as the top tissue, followed by the basal ganglia, breast, lung, and cerebral cortex based on Human Protein Atlas GTEx (Genotype-Tissue Expression) data (RNA-seq data on RSEMv1.2.22 (v7)). In addition, the PITPNC1 protein is a soluble PITP and unique for its high binding affinity with phosphatidic acid (PA), but its functional significance has just started to be studied [27,52]. Recently, *PITPNC1* was found to be highly expressed in omental metastatic lesions of gastric cancer and upregulated by omental adipocytes [53], indicating that it might influence the association between obesity and cancers. Moreover, GWAS identified the single nucleotide polymorphism (SNP): rs8866 as a *PITPNC1* expression-associated risk locus for type 2 diabetes [54]. Here, we found that *PITPNC1* was highly expressed in visceral (omental) adipose tissue, positively correlated with central obesity, and epigenetically suppressed by *HOTAIR* during *in vitro* abdominal adipogenesis. Therefore, our data propose a new genetic mechanism through the *HOTAIR*/*PITPNC1* pathway in which relatively low *HOTAIR* expression in visceral fat depots might allow the dynamic increase in *PITPNC1* to promote ectopic lipid accumulation with subsequent development of insulin resistance and type 2 diabetes. However, further *in vivo* animal or human genetic studies are still required to validate this hypothesis.

Our data showed that *HOTAIR* is likely a functional lncRNA for regulating abdominal adipogenesis. It is not surprising that other lncRNAs might also involve in the pathophysiological process of obesity. Liu et al. [55] had identified several lncRNAs differentially expressed in abdominal SATs between obese and non-obese children and that is correlated with central obesity. Among the differentially expressed lncRNAs that were reported, we specifically measured two children obesity-upregulated lncRNAs *RP11-20G13.3* and *LINC00968* and two children obesity-downregulated lncRNAs *GYG2P1* and *OLMALINC* in our abdominal SATs of normal-weighted and severely obese adults. Intriguingly, we also identified *LINC00968* was significantly increased and *OLMALINC* was considerably downregulated in the obese abdominal SAT. Whereas *RP11-20G13.3* levels showed a non-significant trend of increase and there is no difference of *GYG2P1* expression in the obese abdominal SAT (Supplementary Figure 7B). Overall, our experiments on revisiting these lncRNAs also support that these lncRNAs consistently showed clear changes of expression as they had been reported between obese and normal Abd SAT.

In conclusion, our study indicates that *HOTAIR* is an important epigenetic marker with relatively low expression in the ventral and anterior body areas. Abdominal aberrant overexpression of *HOTAIR* strongly suppresses adipogenesis via intricate DNA methylation, histone modification, and transcriptional regulation of genes associated with nervous system development and lipid metabolism, such as *SLITRK4* and *PITPNC1*. Further understanding and targeting of these *HOTAIR*-downstream molecular pathways may lead to the discovery of novel therapies for ameliorating obesity-associated central fat accumulation and insulin resistance.

4. MATERIALS AND METHODS

4.1. Collection of paired adipose tissue samples

The criteria for inclusion were as follows: individuals aged 20—80 years received cosmetic surgery or elective operations, including bariatric surgery due to morbid obesity or arteriovenous shunting surgery due to end-stage renal disease. The exclusion criteria were pregnancy, current acute illness of cerebrovascular accident, myocardial infarction, heart failure, or psychiatric diseases. Paired adipose tissue samples were collected based on the accessibility of operations, and all participants signed informed consent before participating in this study with agreement to the use of relevant personal information on a confidential basis. Ethical approval was granted by the Tri-Service General Hospital Ethics Committee (TSGHIRB: 2-108-05-052).

4.2. Anthropometric measurements and dual-energy X-ray absorptiometry

Body weight was measured on a standard scale to the nearest 0.1 kg, and standing height was detected using a wall-mounted stadiometer to the nearest 0.1 cm as a barefoot while wearing light indoor clothing. Waist circumference was measured at the midway horizontal plane between the inferior margin of the last rib and the crest of the ilium, and hip circumference was measured at its widest point. Waist and hip circumferences were also detected to the nearest 0.1 cm. The waist-to-hip circumference ratio and body mass index (BMI) were calculated. BMI was calculated as weight in kilograms divided by the square of height in metres. Blood pressure measurement was performed twice in a sitting position after resting for 5 min with at least 1 min separation, and the average value was used as the data presentation. Whole and regional body adiposity was measured using dual-energy X-ray absorptiometry (DXA) as the standard protocol mentioned before [56]

4.3. Measurement of biochemical data

Venous blood samples were drawn under fasting status for at least 8 h. Serum levels of total cholesterol, triglycerides, high-density lipoprotein, low-density lipoprotein, blood urea nitrogen (BUN), creatinine, aspartate aminotransferase (AST), alanine aminotransferase (ALT), and uric acid were measured on a Beckman Synchron LX20 analyser (LX20; Beckman Coulter, Brea, CA, USA). Fasting glucose was measured in the plasma using the glucose oxidase method on a Beckman Glucose Analyzer II (Beckman Instruments, Fullerton, CA, USA). HbA1c was measured using ion-exchange HPLC on an HLC-723G11 instrument.

4.4. Generation of constitutive *HOTAIR* overexpression abdominal preadipocytes

The immortalized abdominal preadipocyte cell line was given by the Metabolic Research Group in the Oxford Centre for Diabetes, Endocrinology and Metabolism [23]. For overexpression of *HOTAIR*, *HOTAIR2* (NR_003716) from the LZRS-*HOTAIR* plasmid (Addgene plasmid #26110) was cloned into the pEGFP-Lv105 vector (Capital Biosciences). pEGFP-Lv105 empty vector was used as a control. Then, ViraPower™ lentiviral packaging mix (Invitrogen) was used to produce

lentiviral particles in HEK293 cells. Immortalized abdominal preadipocytes were transduced with lentiviral particles in 8 μg/ml hexadimethrine bromide (Sigma)-containing growth medium for 20 h. Then, the virus-transduced cells were revived in normal growth medium for an additional 24−28 h with subsequent selection in a puromycin (1−2 μg/ml)-containing growth medium.

4.5. Culture and differentiation of immortalized preadipocytes

The reagent compositions of the growth medium and adipogenic differentiation medium were as previously described [23]. For adipogenesis, immortalized preadipocytes were cultured in growth medium first. Then, two days after full confluence (differentiation day 0), the cells were treated with adipogenic differentiation medium for 14 days as previously described [23].

4.6. Oil red O staining to evaluate the status of adipogenesis

Four percent paraformaldehyde was used to fix day 14 differentiated preadipocytes for 30 min, followed by incubation with 60% isopropanol for 5 min. Then, a 3 mg/ml solution of oil red O was prepared in isopropanol at a final concentration of 60% as the working solution and filtered (0.8 μm, Millipore, Watford, UK). The filtered working solution was added to the cells for 5 min at room temperature, and then, the cells were gently rinsed three times with PBS and photographed using an inverted phase contrast microscope with a camera.

4.7. Gene expression analysis

TRIzol reagent was used to extract total RNA from cells following the manufacturer's protocol. cDNA synthesis was performed using a cDNA synthesis kit (ABI). Quantitative real-time PCR was performed using SYBR green master mix (BIOLINE) in a 7500-FAST PCR machine (ABI). The ΔCT values of the target genes were normalized to the ΔCt of stably expressed reference transcripts (*GAPDH*) [57]. The primer sequences used here are listed in Supplementary Table 5.

4.8. Reduced representation bisulfite sequencing (RRBS)

4.8.1. Genomic DNA was extracted using the GenEluteTM mammalian genomic DNA miniprep kit

(Sigma), and RRBS libraries were constructed using the Ovation® RRBS Methyl-Seq with TrueMethyl® oxBS preparation kit. The streamlined workflow consists of five main steps: MspI digestion, adaptor ligation, final repair, bisulfite conversion, and PCR amplification. The libraries are sequenced after PCR amplification. The reads were then aligned to the human hg19 reference genome and called the methylation level by using BS Seeker2. The uniquely mapped reads were retained for downstream analysis. To calculate the bisulfite conversion rates, the trimmed reads were also aligned to the λ phage genome. The bisulfite conversion rates of each sample were 100% minus the methylation level called by BS Seeker2. To generate genome-wide DNA methylation profiles, we calculated the methylation level for each covered cytosine in the genome. As bisulfite treatment converted unmethylated cytosines (Cs) to thymines (Ts), we estimated the methylation level at each cytosine by #C/(#C + #T), where #C is the number of methylated reads and #T is the number of unmethylated reads. The methylation level per cytosine serves as an estimate of the percentage of cells that are methylated at this cytosine. In this study, we included only cytosines that were covered by at least 4 reads for the analysis. To identify differentially methylated regions (DMRs), a nonoverlapping tiling window approach was used for genome-wide screening. Genomic regions of 500 bp containing more than 4 RRBS-covered CpG sites covered by at least 4 reads in all compared samples were surveyed. A region was deemed differentially methylated if it showed a ≥25% difference in methylation level between Abd *HOTAIR-OE* and Control cells in average methylation level and a t-test p value < 5%. A gene is considered differentially methylated (DMG) if it contains one or more DMRs in the promoter (−1500 bp to +500 bp of transcription start site) or gene body.

4.9. RNA-sequencing

Poly-T oligo-attached beads were used to purify and fragment mRNA for cDNA synthesis. Then, a single 'A' nucleotide was added to the 3′ end of ds cDNA, and multiple indexing adaptors were ligated to 5′ and 3′ of the ends of ds cDNA, followed by PCR amplification, library quality validation (Agilent 2100 Bioanalyzer and Real-Time PCR system) and Illumina NextSeq sequencing. mRNA reads were aligned to the human reference genome (hg19) using HISAT2 [58]. The annotation/normalization of the raw RNA-seq data was performed using Cuffdiff. The differentially expressed genes (DEGs) were defined as a t-test p value < 5% with fold change ≧ 2 and △ FPKM ≧ 0.1 between Abd *HOTAIR-OE* and Control cells.

4.10. RNA immunoprecipitation (RIP)

An EZ-Nuclear RIP (Cross-Linked) kit (Cat#17-10521, Millipore) was used to perform RIP experiments. Formaldehyde (0.3%) was added to the cells (1 × 106/RIP) for 10 min to achieve *in vivo* cross linking. The cross-linked chromatin was incubated on ice and fragmented under frequent vortexing for 30 min. Chromatin supernatant (10%) was collected as the input before adding the following immunoprecipitation antibodies: anti-EZH2 (Cat# CS203195, Millipore) and mouse IgG (Cat# CS200621, Millipore). Magna ChIP Protein A/G Magnetic Beads (Cat# CS207374, Millipore) were utilized to bind the antibody/protein/RNA complex. RIP samples were washed, crosslinks were reversed, and RIP RNA was purified. cDNA was synthesized for real-time qPCR using SYBR Green. To assess the interaction between *HOTAIR* and EZH2, *HOTAIR* primers are listed in Supplementary Table 5.

4.11. Chromatin immuno precipitation (ChIP)

An EZ-Magna ChIP™ Chromatin Immunoprecipitation kit (Cat#17-10086, Millipore) was used to perform ChIP experiments. Then, 1% formaldehyde was added to the cells (3×10^6/ChIP) for 10 min to achieve *in vivo* cross linking. Sonication (30 s ON/OFF for 10 min in a Bioruptor UCD-200, Diagenode) of the cross-linked chromatin was performed to generate <500 bp DNA fragments. Chromatin supernatant (1%) was collected as the input before adding the following immunoprecipitating antibodies: ChIPAb + H3K27me3 (Cat#17-622, Millipore) or mouse IgG (Cat#12-371B, Millipore). Magnetic Protein A/G Beads (Cat# CS204457, Millipore) were used to bind the antibody/antigen/DNA complex. ChIP samples were washed, crosslinks were reversed, and ChIP DNA was isolated as the template for real-time qPCR using SYBR Green. To assess the occupancy of H3K27me3 on the promoter regions of the *SLITRK4*, *PITPNC1*, and *PPARG* genes, the primers are listed in Supplementary Table 5.

DATA AVAILABILITY

The sequence data obtained in this study have been submitted to the NCBI Gene Expression Omnibus (GEO) under GEO accession GSE186159.

FUNDING SOURCES

This work was supported by research grants from Academia Sinica and the Ministry of Science and Technology (MOST 108-2314-B-016 -019 -MY3, MOST 108-2313-B-001 -013 -MY3, MOST 109-2314-B-016 -033, MOST 109-2313-B-001 -009 -MY3, MOST 110-2314-B-016 -022, MOST 110-2314-B-016 -002 -MY3) and Tri-Service General Hospital (TSGH-C04-109030, TSGH-C03-110024, TSGH-PH-E-109006, TSGH-PH-E-110012), and Taichung Armed Forces General hospital (TCAFGH-E-110051) in Taiwan.

AUTHOR CONTRIBUTIONS

FC Kuo and PY Chen conceived and designed the study; FC Kuo, CH Lee, KF Hsu, HY Yang, LW Wu, CH Lu and YJ Hsu curated the data; FC Kuo, YC Huang, MR Yen and PY Chen performed the data analysis and statistical analyses; FC Kuo and YC Huang wrote the original draft; and YC Huang, MR Yen, PY Chen and FC Kuo reviewed and edited the manuscript.

ACKNOWLEDGEMENTS

We thank Prof. Fredrik Karpe at Oxford Centre for Diabetes, Endocrinology and Metabolism for sending us the human immortalized preadipocytes. We are grateful to Dr. Ming-Jin Yang (Asir Clinic, Taipei, Taiwan) for collecting paired human adipose tissues during cosmetic surgery and thank the Genomics BioSci. & Tech. for RNA sequencing services; the Tri-I Biotech, Inc. for reduced representation bisulfite sequencing.

CONFLICT OF INTEREST

The authors declare no competing interests.

APPENDIX A. SUPPLEMENTARY DATA

Supplementary data to this article can be found online at https://doi.org/10.1016/j.molmet.2022.101473.

REFERENCES

[1] Bluher, M., 2019. Obesity: global epidemiology and pathogenesis. Nature Reviews Endocrinology 15(5):288—298.
[2] Chooi, Y.C., Ding, C., Magkos, F., 2019. The epidemiology of obesity. Metabolism 92:6—10.
[3] Emdin, C.A., Khera, A.V., Natarajan, P., Klarin, D., Zekavat, S.M., Hsiao, A.J., et al., 2017. Genetic association of waist-to-hip ratio with cardiometabolic traits, type 2 diabetes, and coronary heart disease. JAMA 317(6):626—634.
[4] Yusuf, S., Hawken, S., Ôunpuu, S., Bautista, L., Franzosi, M.G., Commerford, P., et al., 2005. Obesity and the risk of myocardial infarction in 27,000 participants from 52 countries: a case-control study. Lancet 366(9497):1640—1649.
[5] Karpe, F., Pinnick, K.E., 2015. Biology of upper-body and lower-body adipose tissue–link to whole-body phenotypes. Nature Reviews Endocrinology 11(2):90—100.
[6] Pinnick, K.E., Nicholson, G., Manolopoulos, K.N., McQuaid, S.E., Valet, P., Frayn, K.N., et al., 2014. Distinct developmental profile of lower-body adipose tissue defines resistance against obesity-associated metabolic complications. Diabetes 63(11):3785—3797.
[7] Ye, R.Z., Richard, G., Gévry, N., Tchernof, A., Carpentier, A.C., 2021. Fat cell size: measurement methods, pathophysiological origins, and relationships with metabolic dysregulations. Endocr Rev.
[8] Gehrke, S., Brueckner, B., Schepky, A., Klein, J., Iwen, A., Bosch, T.C., et al., 2013. Epigenetic regulation of depot-specific gene expression in adipose tissue. PLoS One 8(12):e82516.
[9] Karastergiou, K., Fried, S.K., Xie, H., Lee, M.J., Divoux, A., Rosencrantz, M.A., et al., 2013. Distinct developmental signatures of human abdominal and gluteal subcutaneous adipose tissue depots. The Journal of Cinical Endocrinology and Metabolism 98(1):362—371.
[10] Passaro, A., Miselli, M.A., Sanz, J.M., Dalla Nora, E., Morieri, M.L., Colonna, R., et al., 2017. Gene expression regional differences in human subcutaneous adipose tissue. BMC Genomics 18(1):202.
[11] Tsai, M.C., Manor, O., Wan, Y., Mosammaparast, N., Wang, J.K., Lan, F., et al., 2010. Long noncoding RNA as modular scaffold of histone modification complexes. Science 329(5992):689—693.
[12] Chen, Y., Kim, J., Zhang, R., Yang, X., Zhang, Y., Fang, J., et al., 2016. Histone demethylase LSD1 promotes adipocyte differentiation through repressing Wnt signaling. Cell Chemistry Biology 23(10):1228—1240.
[13] Wang, L., Jin, Q., Lee, J.E., Su, I.H., Ge, K., 2010. Histone H3K27 methyltransferase Ezh2 represses Wnt genes to facilitate adipogenesis. Proceedings of the National Academy of Sciences of the United States of America 107(16):7317—7322.
[14] Gupta, R.A., Shah, N., Wang, K.C., Kim, J., Horlings, H.M., Wong, D.J., et al., 2010. Long non-coding RNA HOTAIR reprograms chromatin state to promote cancer metastasis. Nature 464(7291):1071—1076.
[15] Zhang, J., Zhang, P., Wang, L., Piao, H.L., Ma, L., 2014. Long non-coding RNA HOTAIR in carcinogenesis and metastasis. Acta Biochimica et Biophysica Sinica 46(1):1—5.
[16] Shungin, D., Winkler, T.W., Croteau-Chonka, D.C., Ferreira, T., Locke, A.E., Mägi, R., et al., 2015. New genetic loci link adipose and insulin biology to body fat distribution. Nature 518(7538):187—196.
[17] Peng, Y., Li, S., Onufriev, A., Landsman, D., Panchenko, A.R., 2021. Binding of regulatory proteins to nucleosomes is modulated by dynamic histone tails. Nature Communications 12(1):5280.
[18] Seo, S.I., Yoon, J.H., Byun, H.J., Lee, S.K., 2021. HOTAIR induces methylation of PCDH10, a tumor suppressor gene, by regulating DNMT1 and sponging with miR-148b in gastric adenocarcinoma. Yonsei Medical Journal 62(2):118—128.
[19] Song, H., Chen, L., Liu, W., Xu, X., Zhou, Y., Zhu, J., et al., 2021. Depleting long noncoding RNA HOTAIR attenuates chronic myelocytic leukemia progression by binding to DNA methyltransferase 1 and inhibiting PTEN gene promoter methylation. Cell Death & Disease 12(5):440.
[20] Song, B.Q., Chi, Y., Li, X., Du, W.J., Han, Z.B., Tian, J.J., et al., 2015. Inhibition of notch signaling promotes the adipogenic differentiation of mesenchymal stem cells through autophagy activation and PTEN-PI3K/AKT/mTOR pathway. Cellular Physiology and Biochemistry 36(5):1991—2002.
[21] Ye, M., Li, J., Gong, J., 2017. PCDH10 gene inhibits cell proliferation and induces cell apoptosis by inhibiting the PI3K/Akt signaling pathway in hepatocellular carcinoma cells. Oncology Reports 37(6):3167—3174.
[22] Divoux, A., Karastergiou, K., Xie, H., Guo, W., Perera, R.J., Fried, S.K., et al., 2014. Identification of a novel lncRNA in gluteal adipose tissue and evidence for its positive effect on preadipocyte differentiation. Obesity 22(8):1781—1785.
[23] Todorcevic, M., Hilton, C., McNeil, C., Christodoulides, C., Hodson, L., Karpe, F., et al., 2017. A cellular model for the investigation of depot specific human adipocyte biology. Adipocyte 6(1):40—55.
[24] Subuddhi, A., Kumar, M., Majumder, D., Sarkar, A., Ghosh, Z., Vasudevan, M., et al., 2020. Unraveling the role of H3K4 trimethylation and lncRNA HOTAIR in

SATB1 and DUSP4-dependent survival of virulent Mycobacterium tuberculosis in macrophages. Tuberculosis 120:101897.

[25] Wasson, C.W., Abignano, G., Hermes, H., Malaab, M., Ross, R.L., Jimenez, S.A., et al., 2020. Long non-coding RNA HOTAIR drives EZH2-dependent myofibroblast activation in systemic sclerosis through miRNA 34a-dependent activation of NOTCH. Annals of the Rheumatic Diseases 79(4): 507–517.

[26] Kramer, A., Green, J., Pollard Jr., J., Tugendreich, S., 2014. Causal analysis approaches in ingenuity pathway analysis. Bioinformatics 30(4):523–530.

[27] Ashlin, T.G., Blunsom, N.J., Cockcroft, S., 2021. Courier service for phosphatidylinositol: PITPs deliver on demand. Biochim Biophys Acta Mol Cell Biol Lipids 1866(9):158985.

[28] Proenca, C.C., Gao, K.P., Shmelkov, S.V., Rafii, S., Lee, F.S., 2011. Slitrks as emerging candidate genes involved in neuropsychiatric disorders. Trends in Neurosciences 34(3):143–153.

[29] Scarlett, D.J., Herst, P.M., Berridge, M.V., 2005. Multiple proteins with single activities or a single protein with multiple activities: the conundrum of cell surface NADH oxidoreductases. Biochimica et Biophysica Acta 1708(1):108–119.

[30] Lu, C., Kasik, J., Stephan, D.A., Yang, S., Sperling, M.A., Menon, R.K., 2001. Grtp1, a novel gene regulated by growth hormone. Endocrinology 142(10): 4568–4571.

[31] Ghoshdastider, U., Popp, D., Burtnick, L.D., Robinson, R.C., 2013. The expanding superfamily of gelsolin homology domain proteins. Cytoskeleton (Hoboken) 70(11):775–795.

[32] Somarowthu, S., Legiewicz, M., Chillón, I., Marcia, M., Liu, F., Pyle, A.M., 2015. HOTAIR forms an intricate and modular secondary structure. Molecular Cell 58(2):353–361.

[33] Cao, R., Zhang, Y., 2004. The functions of E(Z)/EZH2-mediated methylation of lysine 27 in histone H3. Current Opinion in Genetics & Development 14(2): 155–164.

[34] Scott, M.P., 1992. Vertebrate homeobox gene nomenclature. Cell 71(4):551–553.

[35] Carroll, S.B., 1995. Homeotic genes and the evolution of arthropods and chordates. Nature 376(6540):479–485.

[36] Pearson, J.C., Lemons, D., McGinnis, W., 2005. Modulating Hox gene functions during animal body patterning. Nature Reviews Genetics 6(12):893–904.

[37] Cantile, M., Di Bonito, M., Tracey De Bellis, M., Botti, G., 2021. Functional interaction among lncRNA HOTAIR and MicroRNAs in cancer and other human diseases. Cancers 13(3).

[38] Yoon, J.H., Abdelmohsen, K., Kim, J., Yang, X., Martindale, J.L., Tominaga-Yamanaka, K., et al., 2013. Scaffold function of long non-coding RNA HOTAIR in protein ubiquitination. Nature Communications 4:2939.

[39] Özeş, A.R., Miller, D.F., Özeş, O.N., Fang, F., Liu, Y., Matei, D., et al., 2016. NF-kappaB-HOTAIR axis links DNA damage response, chemoresistance and cellular senescence in ovarian cancer. Oncogene 35(41):5350–5361.

[40] Price, R.L., Bhan, A., Mandal, S.S., 2021. HOTAIR beyond repression: in protein degradation, inflammation, DNA damage response, and cell signaling. DNA Repair 105:103141.

[41] Gao, S., Guo, X., Zhao, S., Jin, Y., Zhou, F., Yuan, P., et al., 2019. Differentiation of human adipose-derived stem cells into neuron/motoneuron-like cells for cell replacement therapy of spinal cord injury. Cell Death & Disease 10(8): 597.

[42] Guilherme, A., Henriques, F., Bedard, A.H., Czech, M.P., 2019. Molecular pathways linking adipose innervation to insulin action in obesity and diabetes mellitus. Nature Reviews Endocrinology 15(4):207–225.

[43] Morrison, S.F., Madden, C.J., 2014. Central nervous system regulation of brown adipose tissue. Comprehensive Physiology 4(4):1677–1713.

[44] Charo, N.L., Rodríguez Ceschan, M.I., Galigniana, N.M., Toneatto, J., Piwien-Pilipuk, G., 2016. Organization of nuclear architecture during adipocyte differentiation. Nucleus 7(3):249–269.

[45] Khan, A.U., Qu, R., Fan, T., Ouyang, J., Dai, J., 2020. A glance on the role of actin in osteogenic and adipogenic differentiation of mesenchymal stem cells. Stem Cell Research & Therapy 11(1):283.

[46] Marquez, M.P., Alencastro, F., Madrigal, A., Jimenez, J.L., Blanco, G., Gureghian, A., et al., 2017. The role of cellular proliferation in adipogenic differentiation of human adipose tissue-derived mesenchymal stem cells. Stem Cells and Development 26(21):1578–1595.

[47] Rodriguez-Acebes, S., Palacios, N., Botella-Carretero, J.I., Olea, N., Crespo, L., Peromingo, R., et al., 2010. Gene expression profiling of subcutaneous adipose tissue in morbid obesity using a focused microarray: distinct expression of cell-cycle- and differentiation-related genes. BMC Medical Genomics 3:61.

[48] Malodobra-Mazur, M., Cierzniak, A., Kaliszewski, K., Dobosz, T., 2021. PPARG hypermethylation as the first epigenetic modification in newly onset insulin resistance in human adipocytes. Genes 12(6).

[49] Yin, R., Fang, L., Li, Y., Xue, P., Li, Y., Guan, Y., et al., 2015. Pro-inflammatory macrophages suppress PPARgamma activity in adipocytes via S-nitrosylation. Free Radical Biology and Medicine 89:895–905.

[50] Kang, H., Han, K.A., Won, S.Y., Kim, H.M., Lee, Y.H., Ko, J., et al., 2016. Slitrk missense mutations associated with neuropsychiatric disorders distinctively impair Slitrk trafficking and synapse formation. Frontiers in Molecular Neuroscience 9:104.

[51] Haakensen, V.D., Bjøro, T., Lüders, T., Riis, M., Bukholm, I.K., Kristensen, V.N., et al., 2011. Serum estradiol levels associated with specific gene expression patterns in normal breast tissue and in breast carcinomas. BMC Cancer 11:332.

[52] Garner, K., Hunt, A.N., Koster, G., Somerharju, P., Groves, E., Li, M., et al., 2012. Phosphatidylinositol transfer protein, cytoplasmic 1 (PITPNC1) binds and transfers phosphatidic acid. Journal of Biological Chemistry 287(38):32263–32276.

[53] Tan, Y., Lin, K., Zhao, Y., Wu, Q., Chen, D., Wang, J., et al., 2018. Adipocytes fuel gastric cancer omental metastasis via PITPNC1-mediated fatty acid metabolic reprogramming. Theranostics 8(19):5452–5468.

[54] Greenawalt, D.M., Sieberts, S.K., Cornelis, M.C., Girman, C.J., Zhong, H., Yang, X., et al., 2012. Integrating genetic association, genetics of gene expression, and single nucleotide polymorphism set analysis to identify susceptibility Loci for type 2 diabetes mellitus. American Journal of Epidemiology 176(5):423–430.

[55] Liu, Y., Ji, Y., Li, M., Wang, M., Yi, X., Yin, C., et al., 2018. Integrated analysis of long noncoding RNA and mRNA expression profile in children with obesity by microarray analysis. Scientific Reports 8(1):8750.

[56] Kuo, F.C., Lu, C.H., Wu, L.W., Kao, T.W., Su, S.C., Liu, J.S., et al., 2020. Comparison of 7-site skinfold measurement and dual-energy X-ray absorptiometry for estimating body fat percentage and regional adiposity in Taiwanese diabetic patients. PLoS One 15(7):e0236323.

[57] Neville, M.J., Collins, J.M., Gloyn, A.L., McCarthy, M.I., Karpe, F., 2011. Comprehensive human adipose tissue mRNA and microRNA endogenous control selection for quantitative real-time-PCR normalization. Obesity 19(4): 888–892.

[58] Kim, D., Paggi, J.M., Park, C., Bennett, C., Salzberg, S.L., 2019. Graph-based genome alignment and genotyping with HISAT2 and HISAT-genotype. Nature Biotechnology 37(8):907–915.

